



**HAL**  
open science

## Identification of indoor air quality events using a K-means clustering analysis of gas sensors data

Alexandre Caron, Nathalie Redon, Patrice Coddeville, Benjamin Hanoune

► **To cite this version:**

Alexandre Caron, Nathalie Redon, Patrice Coddeville, Benjamin Hanoune. Identification of indoor air quality events using a K-means clustering analysis of gas sensors data. *Sensors and Actuators B: Chemical*, 2019, *Sensors and Actuators B: Chemical*, 297, pp.126709. 10.1016/j.snb.2019.126709 . hal-02276311

**HAL Id: hal-02276311**

**<https://hal.univ-lille.fr/hal-02276311>**

Submitted on 25 Oct 2021

**HAL** is a multi-disciplinary open access archive for the deposit and dissemination of scientific research documents, whether they are published or not. The documents may come from teaching and research institutions in France or abroad, or from public or private research centers.

L'archive ouverte pluridisciplinaire **HAL**, est destinée au dépôt et à la diffusion de documents scientifiques de niveau recherche, publiés ou non, émanant des établissements d'enseignement et de recherche français ou étrangers, des laboratoires publics ou privés.



Distributed under a Creative Commons Attribution - NonCommercial 4.0 International License

# 1 **Identification of indoor air quality events using a K-means clustering analysis of gas sensors** 2 **data**

3 Alexandre Caron<sup>1,2</sup>, Nathalie Redon<sup>2</sup>, Patrice Coddeville<sup>2</sup>, Benjamin Hanoune<sup>1</sup>

4 1. Univ. Lille, CNRS, UMR 8522 – PC2A – Physicochimie des Processus de Combustion et de  
5 l’Atmosphère, F-59000 Lille, France.

6 2. IMT Lille Douai, Univ. Lille, SAGE - Département Sciences de l’Atmosphère et Génie de  
7 l’Environnement, F-59000 Lille, France.

8 \* Corresponding author: [nathalie.redon@imt-lille-douai.fr](mailto:nathalie.redon@imt-lille-douai.fr)

9 Tel: (+33)3 27 71 24 77

10 Fax: (+33)3 27 71 29 14

11 IMT Lille Douai, SAGE, 941 rue Charles Bourseul, CS10838, F-59508 Douai, France

12

13

## 14 **Abstract:**

15 Commercial miniature gas sensors, because they are smaller and cheaper than conventional  
16 instruments, can be deployed in large numbers to investigate indoor air quality, for research and  
17 operational purposes. To compensate for their limited metrological performances, it is necessary to  
18 develop relevant data treatment procedures. We applied an unsupervised classification approach  
19 based on the bisecting K-means algorithm to data acquired by online gas analyzers and by miniature  
20 sensors during a measurement campaign in a low energy school building. This procedure, applied to  
21 the analyzers measurements, was able to distinguish the ventilation status and the specific air  
22 quality events taking place in the classroom. The same procedure applied to the data from the  
23 sensors, even though they were not calibrated beforehand, was also able to identify the same events.  
24 The good agreement between the two sets of results validates the methodology and opens up new  
25 perspectives for a massive deployment of sensors inside buildings.

26

27 **Key words:** (indoor) air pollution, electronic gas sensors, unsupervised classification, k-means  
28 clustering

## 29 **1. Introduction**

30 Indoor environments, where people in developed countries spend up to 90% of their time, present  
31 high specific pollutant concentrations [1,2], inducing a risk for human health [3,4]. Indoor  
32 pollutants, especially volatile organic compounds (VOCs), are emitted from building materials,  
33 furniture, consumer products, from the occupants themselves and their activities. The air transferred  
34 from outdoors also has a significant impact on the pollutants breathed indoors [5]. There is a need  
35 for large scale and continuous measurements of the indoor air quality (IAQ) in various domains: (i)  
36 for research purposes, in order to increase the understanding of the determinants of indoor air  
37 pollution, such as the identification of pollution sources and of the pollutants trends and temporal  
38 and spatial evolution, (ii) to allow mandatory or voluntary IAQ assessments of buildings, (iii) to  
39 communicate helpful information to the occupants on the relationships between their daily activities  
40 and the induced pollution levels, and also to alert them and implement corrective actions when  
41 critical thresholds are exceeded, (iv) to control the operation of ventilation or air treatment systems  
42 in order to reach the best compromise between health and energy consumption considerations. The  
43 conventional gas analyzers used for laboratory research and regulatory outdoor air monitoring can  
44 be deployed during research oriented measurement campaigns but not for real-time monitoring of  
45 occupied indoor environments. These bulky analyzers generate many nuisances, such as noise or  
46 vibrations, induce a considerable electrical consumption, and are too expensive to be  
47 simultaneously deployed in many places.

48 In recent years, gas micro-sensors emerged as alternative relevant tools for air quality monitoring  
49 [6–9]. New sensitive materials are constantly being developed in order to achieve better sensitivity,  
50 selectivity and stability [10,11]. More and more micro-sensors are commercially available [12,13],  
51 prompting many recent studies where their performances are investigated [14–17]. Among these  
52 sensors, a distinction must be made between intrinsically non-selective sensors and selective or  
53 nearly-selective sensors. Non-selective sensors are commonly based on metal oxide semiconductive  
54 materials which respond to multiple compounds in the air, and are generally used in combinations

55 or arrays of sensors, also known as e-noses. Selective sensors include the electrochemical sensors  
56 targeting compounds such as carbon monoxide, ozone, nitrogen monoxide or dioxide, sulfur  
57 dioxide, hydrogen sulfide, the NDIR sensors used for carbon dioxide, as well as the PID sensors for  
58 total volatile organic compounds measurements. In spite of the technological progresses, the  
59 currently available sensors still require a complete metrological characterization [18], with in  
60 particular the assessment of their reliability over time. Even if they are very sensitive, the response  
61 of most sensors shows interferences with other compounds than the targeted one, depends upon the  
62 temperature and humidity, and drifts with time [19–21]. Such a preliminary step of characterization  
63 and calibration is not necessary for arrays of MOS sensors when used in association with pattern  
64 recognition algorithms [22–27], which are methods used in data mining for the extraction of useful  
65 information and the exploration of data correlation. Supervised classification approaches [28] are  
66 based on a classifier built from a training set with a collection of labeled data, and then used to  
67 assign new unlabeled data instances. Unsupervised classification [29] refers to algorithms that  
68 require no training set (blind partitioning), no a priori knowledge of the structure of the dataset, and  
69 automatically define the different classes. However, the physical meaning of these classes needs to  
70 be a posteriori interpreted or verified by the expert.

71 In the present study, we investigate the potential of unsupervised classification, or clustering, to  
72 analyze the output of selective gas sensors. The dataset used for the analysis has been acquired  
73 during a field campaign aiming to investigate the drivers and dynamics of IAQ in a low energy  
74 building [5].

75 Many clustering algorithms have been developed for data mining, such as reviewed in [29].  
76 Different clustering algorithms, or even different ways to use them on the same dataset, can lead to  
77 different partition results. None of them have proved to be the best technique in a large amount of  
78 configurations. Some of these algorithms have been applied to electronic nose data clustering [30],  
79 each with its respective possibilities and limitations [25,31,32], depending on the application. For

80 electronic nose data, hierarchical clustering is commonly used [33–37]. It results in a hierarchical  
81 structure of the dataset that is more informative about the link between each group of data than the  
82 unstructured clusters provided by other techniques. In addition, its representation (dendrograms)  
83 allows the selection of the number of clusters. Centroid-based algorithms such as K-means [38] are  
84 less considered in the micro gas sensor field [39,40] and especially for air quality investigation,  
85 though K-means is a simple partitional algorithm and one of the most widely used techniques in  
86 data mining thanks to its performances [41]. K-means algorithms combine simplicity, ease of  
87 implementation and of use, speed of convergence, even with a large number of variables and  
88 clusters, and ability to process datasets with missing values. For these reasons, we have chosen this  
89 method to analyze the data from gas sensors in the investigation of indoor air quality.

90

## 91 **2. Materials and methods**

### 92 **2.1. Instruments and measurements settings**

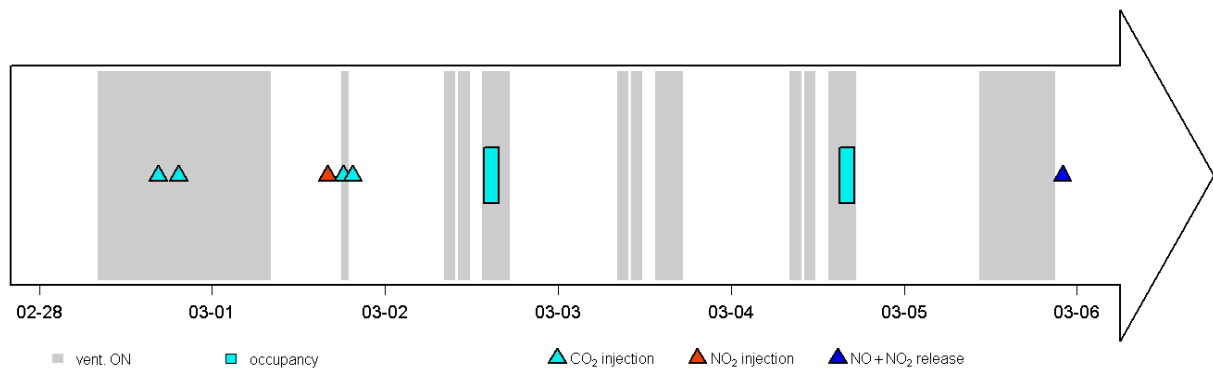
93 Measurements used for this work were performed during the Mermaid study [5]. This field  
94 campaign has been carried out in February and March 2015 in a 51 m<sup>2</sup> (139 m<sup>3</sup>) classroom of an  
95 energy efficient junior high school building in Northern France. Details on the analytical  
96 instruments used for this study can be found in [5]. Only the data from the pollutants from outdoors  
97 (NO<sub>x</sub> and O<sub>3</sub>), measured with online analyzers (Thermo 42i and Thermo 49i), and of CO<sub>2</sub>, measured  
98 with Testo 480 probe located at the center of the room are considered here. In addition to these  
99 instruments, miniature sensors were installed in the center of the classroom, 90 cm above the floor.  
100 They monitor nitrogen oxide (electrochemical, Alphasense NO-B4), nitrogen dioxide  
101 (electrochemical, Alphasense NO<sub>2</sub>-B4), ozone (electrochemical, Alphasense O<sub>3</sub>-B4) and carbon  
102 dioxide (NDIR, Alphasense CO<sub>2</sub>-IRC A1). A Raspberry Pi B+ and an Arduino board are used to  
103 collect, store and transmit the data. No correction or calibration of the sensors has been performed

104 prior to their installation in the room, and the raw output (voltage) is analyzed with the bisecting K-  
105 means procedure.

106

## 107 2.2. Experimental datasets

108 The data used for this work corresponds to a 6-day continuous measurement (28 February 2015 to 6  
109 March 2015). Fig. 1 presents the ventilation status and specific events taking place in the room  
110 during this period. These events include three CO<sub>2</sub> injections with ventilation ON, one CO<sub>2</sub>  
111 injection with ventilation OFF, for the determination of the air exchange rate of the room, two  
112 periods with people in the room, one NO<sub>2</sub> injection, and an accidental release of both NO and NO<sub>2</sub>.



113

114 **Fig. 1.** Specific conditions and events occurring in the classroom

115

116 Dataset 1 (reference instruments) is a 4 x 8160 matrix consisting of 4 variables which are the  
117 concentrations of ozone, nitrogen oxide and nitrogen dioxide (in ppb) measured by the online  
118 analyzers and of carbon dioxide concentration (in ppm) measured by the Testo 480 probe, with a  
119 one minute resolution. The analyzers and CO<sub>2</sub> probe were calibrated at the beginning of the  
120 campaign.

121 Dataset 2 (electrochemical and NDIR sensors) is also a 4 x 8160 matrix, consisting of the voltage  
122 (mV) outputs of the 3 electrochemical sensors and of the carbon dioxide concentration (in ppm)

123 provided by the NDIR sensor, with a 1 min resolution. As previously mentioned, no correction or  
124 calibration of the sensors signals was performed.

125

### 126 **2.3 K-means implementation**

127 Numerous extensions of the basic K-means algorithm have been developed in order to improve its  
128 partitioning abilities for dedicated applications. Classical K-means performs a direct classification  
129 of the full dataset into a number of K clusters, whereas other methods, such as the bisecting K-  
130 means method [38], use a hierarchical method and split the data by iteration. In 2000, Steinbach et  
131 al. have shown that bisecting K-means, computed as an hybrid approach between the run-time  
132 efficiency of conventionnal K-means and the quality efficiency of an agglomerative hierarchical  
133 clustering, has higher performances than the conventional algorithm [44]. It as also been  
134 demonstrated that bisecting K-means is relatively insensitive to the initialisation of the clusters  
135 centers and has a higher computational efficiency than the conventional K-means algorithm [45]. In  
136 spite of its simplicity, and of its wide use, the reasons behind the efficiency of the K-means  
137 algorithm still need to be fully understood. The only required input from the user is the number of  
138 clusters into which the dataset must be split. In the present work, we used the K-means procedure  
139 with a program written in Julia 0.4.0.

140 The raw time series data of each dataset is used for input, except for the carbon dioxide  
141 concentration, measured either by the Testo probe or the NDIR sensor, for which the logarithm  
142 (base 10) is used, because of the much wider range over which this concentration can vary.  
143 Preliminary calculations, not reported here, with the direct CO<sub>2</sub> concentration, were performed but  
144 the clustering was less efficient than with the log values.

145 The only other parameter for input is the number K of clusters. Values of K ranging from 2 to 10  
146 have been investigated for each dataset. Some mathematical criteria to determine the optimal

147 number of clusters have been proposed [44–46], but these may have no physical meanings, and we  
148 have chosen to leave this determination to the judgment of the expert a posteriori.

149 The program first normalizes all the observations in the dataset, in order to standardize their  
150 respective weight on the cluster partition. The clustering process is then initialized by splitting the  
151 normalized dataset into two subsets. Then, each datapoint is assigned to its nearest cluster center  
152 (centroid) according to the euclidian distance. The process is repeated until the association of all the  
153 observations of the dataset to its respective cluster does not change anymore and the sum of the  
154 squared errors of the distance is minimized. The process is iterated by splitting into two new  
155 clusters the cluster with the highest sum of squared residuals, following the same procedure, until  
156 the required number of clusters is reached. Tests have shown that changing the initial partition does  
157 not influence the final results. The output file of the bisecting K-means clustering consists of the  
158 raw data tagged with their respective cluster, and of the coordinates of the centroids of each of the K  
159 clusters.

160 To compare the outputs of the K-means procedure applied to the two dataset (reference dataset and  
161 sensors dataset), we will consider the overlap ratio between a cluster from dataset 2 and its  
162 equivalent cluster from the reference dataset 1. It is expressed as the number of correct matches  
163 between each datapoint in a defined cluster of each dataset normalized by the number of data points  
164 in the reference cluster. Thus, a value of 1 indicates a perfect overlap, while a value of 0 means no  
165 overlap between the two clusters.

166

167

168

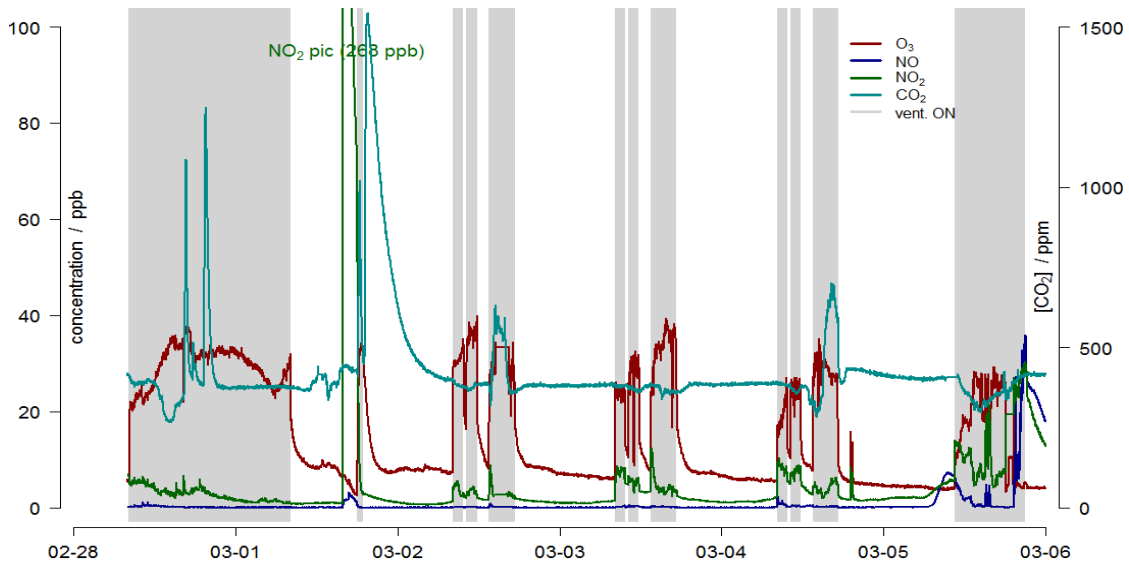
## 169 **3 Results and discussion**

### 170 **3.1 Clustering of the reference online analyzers measurements (dataset 1)**



171 Dataset 1 (concentrations of NO, NO<sub>2</sub>, O<sub>3</sub> and CO<sub>2</sub> measured by the reference instruments) are  
172 presented on Fig. 2, together with the ventilation status (ON/OFF) which has been found to be the  
173 main driver of the chemistry in the room [5]. The specific events described on Fig.1 are clearly  
174 distinguished on the concentration time chart of Fig. 2..

175

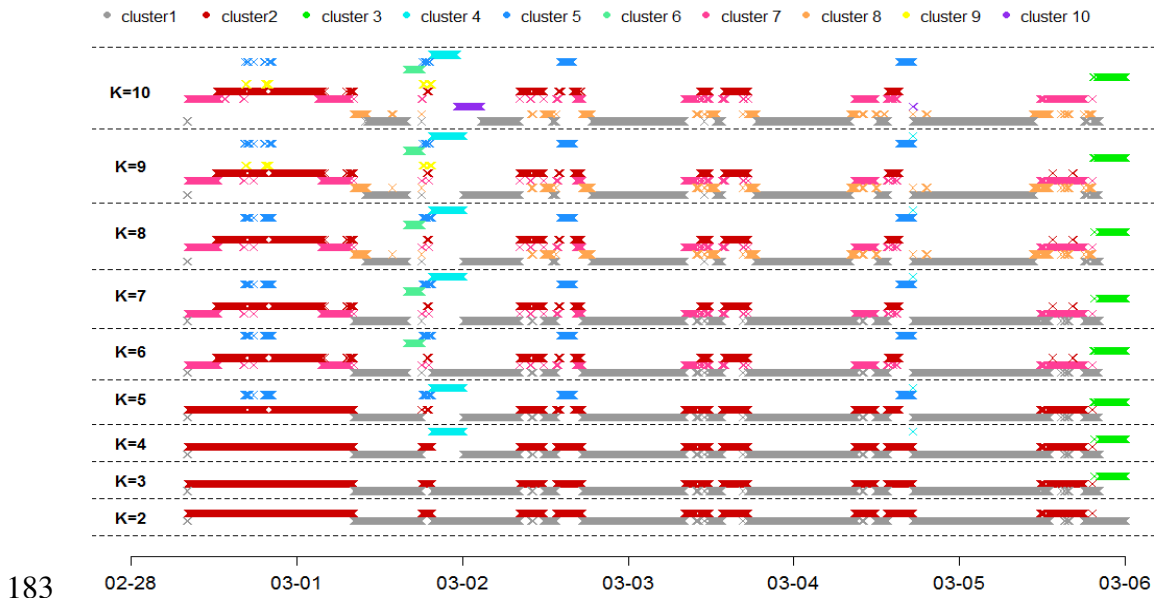


176

177 **Fig. 2.** Concentration time series measured by the reference analyzers. The ventilation status is  
178 indicated by the background color, white for ventilation OFF, grey for ventilation ON.

179

180 The results of the clustering process, applied considering a number of clusters ranging from 2 to 10,  
181 are displayed on Fig. 3. This chart clearly illustrates the hierarchical structure of the bisecting K-  
182 means process.



183  
184 **Fig. 3.** Dataset 1 clustering process output, for K values from 2 to 10

185

186 Data are successively grouped into new clusters, with the 2 clusters divided into smaller sub-  
 187 clusters when K increases. For the initial partition (K=2), the bisecting K-means separates the  
 188 dataset according to the ozone concentration, with cluster 1 corresponding to the periods with no  
 189 ozone, i.e. when the ventilation is OFF, while cluster 2 refers to the periods where the ozone  
 190 concentration is significant, i.e. when the ventilation is ON. This result agrees with the result of the  
 191 MERMAID campaign [5], where the main driver of the IAQ within the room was found to be the  
 192 ventilation status. When K increases from 3 to 5, the newly defined clusters can be related to the  
 193 specific known events occurring in the room presented in Fig. 1. Cluster 3 corresponds to the  
 194 accidental release of NO and NO<sub>2</sub> in the classroom, cluster 4 corresponds to the injection of carbon  
 195 dioxide when the ventilation system is OFF, and cluster 5 corresponds to the moments when the  
 196 ventilation system is ON and with CO<sub>2</sub> concentration higher than the background, due to either  
 197 controlled injection of CO<sub>2</sub> in the room or to human presence.

198 Interestingly, the results for K=6 differ drastically from the previous cases. The new cluster (#6)  
 199 corresponds to the injection of NO<sub>2</sub>, the previously found cluster 4 (injection of CO<sub>2</sub> during  
 200 ventilation OFF conditions) disappears, and cluster 2 (ventilation ON) is divided into two sub-

201 clusters. However, cluster 4 reappears when considering the  $K=7$  partitioning, with no change on  
202 the previously determined clusters. This indicates that a criterion of stability of the clusters when  
203 increasing their number must be considered to correctly interpret the results of unsupervised  
204 classification. Higher values of  $K$  up to 10 induce a refinement in the previously determined  
205 clusters, according to different levels of ozone. Cluster 8 corresponds to the transition period when  
206 the pollutants from outdoor air slowly decrease due to their reactivity, with no compensation from  
207 the ventilation, cluster 9 represents the transient periods with elevated ozone and  $\text{CO}_2$   
208 concentration, and cluster 10 corresponds to a moderate  $\text{CO}_2$  concentration with no ozone. These  
209 transitions periods, and in particular the mixing between indoor and outdoor pollutants, are  
210 generally overlooked during standard analysis.

211 While clusters 8 to 10 correspond to actual, well-defined conditions in the room, their interpretation  
212 is less forward than the previous 7 clusters, and we will consider henceforth that  $K=7$  provides the  
213 best description of the air quality events in the room. A lower  $K$  value will miss some events, and a  
214 higher  $K$  value will only split classes with physical meaning according to the levels of  
215 concentration.  $K=7$  leads to the best compromise between the lowest numbers of cluster and the  
216 correct and separate description of every known event.

217

218 **Table 1** Summary of clusters size and coordinates of centroids for K=7 clustering (dataset 1)

Cluster	Events	n. obs	O <sub>3</sub> / ppb	NO / ppb	NO <sub>2</sub> /ppb	CO <sub>2</sub> /ppm
C1	Vent. OFF	4480	7.7	0.5	2.8	396
C2	Vent. ON	1180	24.4	0.4	5.6	369
C3	Vent. ON	1467	32.4	0.2	3.1	367
C4	NO+NO <sub>2</sub>	228	4.3	23.8	20.5	416
C5	NO <sub>2</sub>	128	4.7	1.9	122.3	435
C6	CO <sub>2</sub> (vent. OFF)	277	9.4	0.1	1.8	965
C7	CO <sub>2</sub> (vent. ON)	400	31.1	0.2	4.0	666

219

220 The output results from the partition of dataset 1 into 7 clusters are presented in Table 1, which  
 221 summarizes the size (number of data points in the cluster) and centroid coordinates of each cluster,  
 222 together with their assignment. Cluster 1 groups the majority of the datapoints, with 4480  
 223 observations, and is characterized by low levels of every pollutant, as it corresponds to the periods  
 224 with no ventilation, i.e. no intake of outdoor pollutants. A high ozone level is the dominant  
 225 parameter that influences cluster 2 (1180 obs.) and cluster 3 (1467 obs.). These two clusters  
 226 correspond to periods when the ozone concentration increases in the classroom due to the activation  
 227 of the ventilation system. Cluster 4 (228 obs.) data are characterized by background CO<sub>2</sub> (416 ppm)  
 228 and O<sub>3</sub> (4.3 ppb) level, together with higher NO and NO<sub>2</sub> levels (> 20 ppb). This partition  
 229 corresponds to the short event that takes place at the end of the measurement period (Fig. 1, Fig. 2)  
 230 which is an accidental release of NO and NO<sub>2</sub>. Cluster 5 (128 obs.) data are characterized by low  
 231 level of pollutants in the classroom, except for NO<sub>2</sub> (112.3 ppb), and corresponds to a voluntary  
 232 injection of nitrogen dioxide in the classroom. Cluster 6 represents the CO<sub>2</sub> injection when the  
 233 ventilation is off, with low O<sub>3</sub>, NO and NO<sub>2</sub> concentrations. Cluster 7 represents the moments with

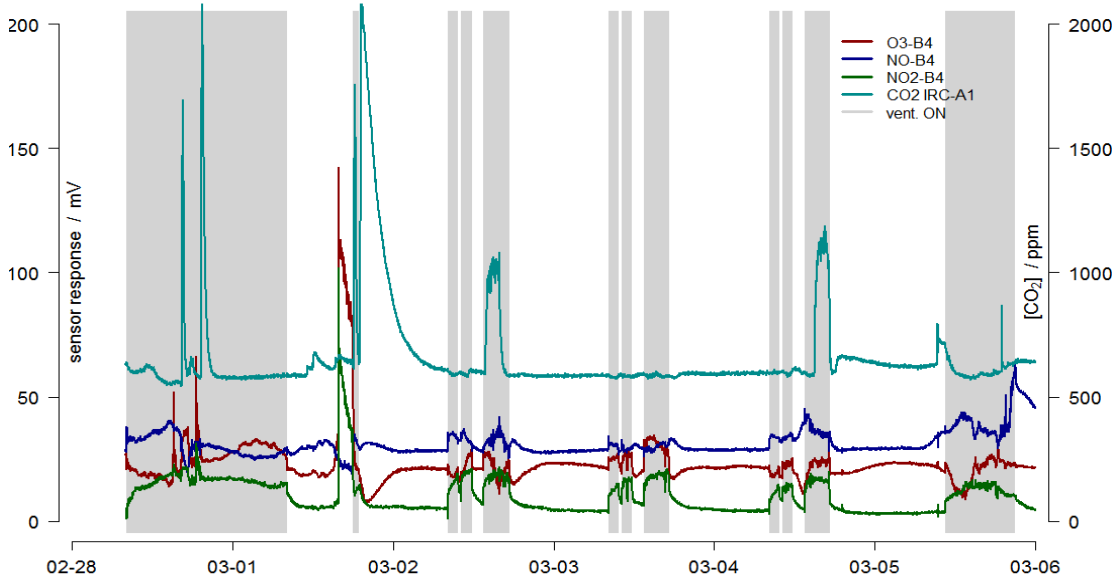
234 high O<sub>3</sub> concentration, that is during ventilation ON, together with high CO<sub>2</sub> concentration, due to  
235 either a CO<sub>2</sub> injection or the presence of people in the room.

236

### 237 3.2 Clustering of the electrochemical and NDIR sensors measurements (dataset 2)

238 The time series evolution of dataset 2 is presented on Fig. 4. The direct interpretation of the signals  
239 from the sensors must be done with caution, because of possible chemical interferences, such as the  
240 cross response of NO<sub>2</sub> and O<sub>3</sub> on electrochemical sensors [47] and because the sensors were not  
241 calibrated before taking the measurements. This is where unsupervised classification algorithms can  
242 really help analyzing the data.

243



244

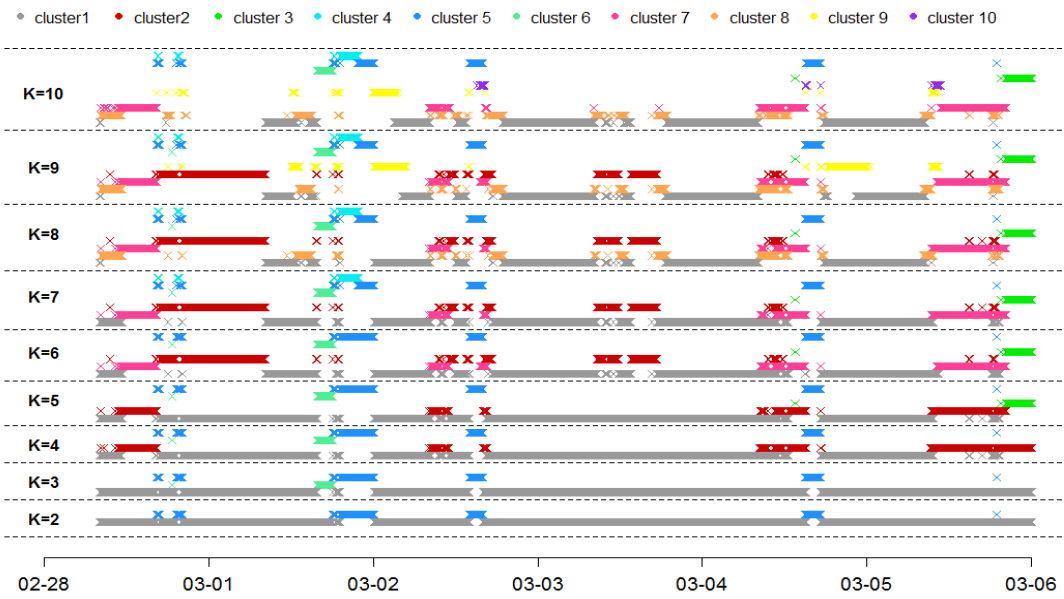
245 **Fig. 4.** Time series of the sensors signals. The ventilation status is indicated by the background  
246 color, white for ventilation OFF, grey for ventilation ON.

247

248 The results of the process for each K value between 2 and 10 are displayed on Fig. 5, illustrating, as  
249 for dataset 1, the hierarchical structure induced by the bisecting K-means process. However, the  
250 different clusters do not appear in the same order as for dataset 1. K=2 separates the datapoints with  
251 high CO<sub>2</sub> concentration. For K=3, the new cluster can be related to the injection of NO<sub>2</sub> in the  
252 classroom. The accidental release of NO and NO<sub>2</sub> is identified in dataset 2 at K=5. The efficiency of

253 the ventilation, impacting the O<sub>3</sub> concentrations (oxydants coming from outdoor), is identified by  
 254 clusters built from K=4 and K=6. At K=6, every known event can be related to a specific cluster,  
 255 except the distinction between the CO<sub>2</sub> injections during the ventilation period or without  
 256 ventilation, which appears only for the classification into 7 clusters. The clusters obtained for  
 257 dataset 2 when increasing the value of K up to 10 are difficult to put in regard to the actual events  
 258 taking place in the room. For instance, cluster 8 cannot be related to any event in the room. Also,  
 259 cluster 9 is not stable, and partly disappears for K=10. Still, as the clusters do not appear in the same  
 260 order when considering the reference dataset or the sensor dataset, it is necessary to explore the  
 261 analysis with high K values, in order not to miss a specific event.

262  
 263  
 264



265  
 266 **Fig. 5.** Dataset 2 (sensors) clustering process output for K values up to 10. To help the comparison  
 267 with the results of dataset 1, the cluster numbering and color coding does not follow the increasing  
 268 K order, but is taken at the K=7 level.

269  
 270 This analysis demonstrates that the bisecting K-means procedure can also be used for sensors, when  
 271 the activities in the room are known, even when the sensors are not calibrated before the

272 experiment. This comes from the fact that the information does not lie in the absolute value of the  
273 measurements, but in the evolution of the intensity of the signals. This holds true also in spite of the  
274 poor selectivity, as in the case of the NO<sub>2</sub> and O<sub>3</sub> sensors. However, the K-means processing of  
275 dataset 2 also points to the difficulty of determining the optimal number of clusters, which in the  
276 present case could be 7 or 8, depending if we consider the physical meaning of the classes, that is if  
277 we use contextual information to supplement the measured data, or 8 if we consider the stability of  
278 the clusters, without contextual information.

279 As discussed when treating previously dataset 1, and considering our goal of comparing the results  
280 obtained from the two datasets, we will restrict hereafter our discussion to K=7. The results from  
281 the partition of dataset 2 into 7 clusters are presented in Table 2, summarizing the size and centroid  
282 coordinates of each cluster. Cluster 1 (4394 obs.) is characterized by a background level of the O<sub>3</sub>-  
283 B4 and NO-B4 response, of respectively 21.2 and 29.54 mV, a background (uncorrected) CO<sub>2</sub>  
284 concentration value of 614 ppm, and a low NO<sub>2</sub>-B4 value of 5.8 mV. This partition matches well  
285 with the period when the ventilation is turned off. Cluster 2 (1246 obs.) is characterized by a higher  
286 response from the NO-B4 sensor (37.20 mV) and from the NO<sub>2</sub>-B4 sensor (13.90 mV). Cluster 3  
287 (1515 obs.) is characterized by a higher response from the three electrochemical sensors. Both  
288 cluster 2 and cluster 3 describe the period where the outdoor pollutant contribution is significant,  
289 and can be related to the ventilation ON status. The two clusters differ by the higher values of O<sub>3</sub> in  
290 cluster 3. Cluster 4 (225 obs.) mainly appears at the end of the measurement period and is  
291 characterized by a significant increase of NO-B4 sensor response (51.49 mV). It corresponds to the  
292 simultaneous increase of NO and NO<sub>2</sub> concentration. Cluster 5 (129 obs.) corresponds to the  
293 maximal values from the O<sub>3</sub>-B4 and NO<sub>2</sub>-B4 sensors, respectively of 95.6 mV and 49.3 mV. This  
294 data partition can be linked to the injection of nitrogen dioxide into the room. Clusters 6 (208 obs.)  
295 and 7 (443 obs.) data match with the high CO<sub>2</sub> concentration periods, with (uncorrected)  
296 concentrations of 1658 and 1035 ppm respectively.

298 **Table 2** Summary of clusters size and coordinates of centroids for K=7 clustering (dataset 2)

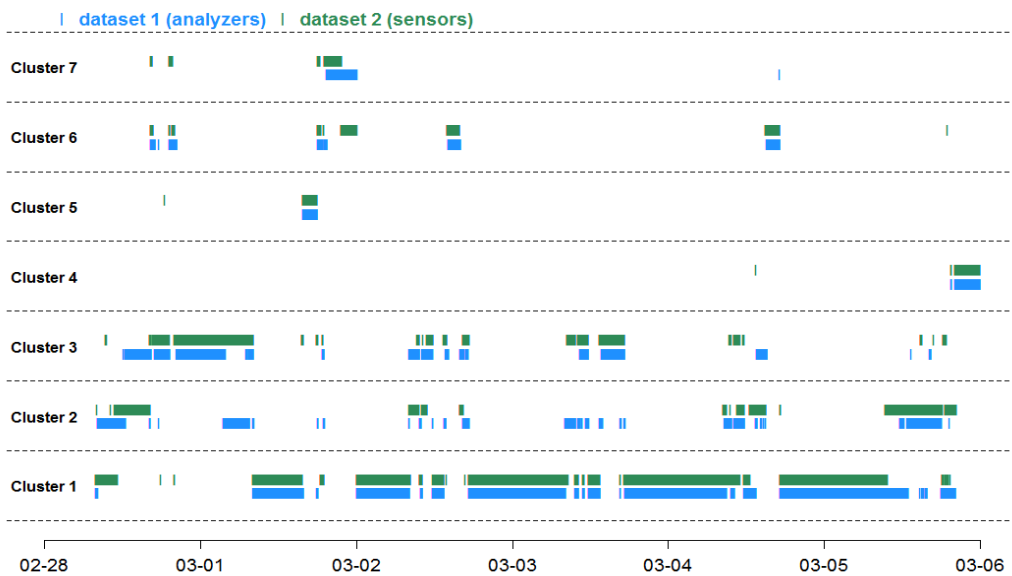
Cluster	Events	n. obs	O <sub>3</sub> -B4/ mV	NO-B4 / mV	NO <sub>2</sub> -B4/mV	CO <sub>2</sub> IRC-A1/ppm
C1	Vent. OFF	4394	21.20	29.54	5.80	614
C2	Vent. ON	1246	19.19	37.20	13.90	601
C3	Vent. ON	1515	28.32	28.82	16.53	592
C4	NO+NO <sub>2</sub>	225	22.13	51.49	7.34	642
C5	NO <sub>2</sub>	129	95.63	22.23	49.28	650
C6	CO <sub>2</sub> (vent. OFF)	208	14.22	31.09	9.39	1658
C7	CO <sub>2</sub> (vent. ON)	443	21.26	32.48	13.65	1035

299

300 **3.3 Comparison of both clustering results**

301 Fig. 6 depicts graphically the clusters obtained from the two datasets. The overlap between the two  
302 sets of clusters is summarized in Table 3 (percentage of datapoints from each cluster from the  
303 sensors dataset that are assigned to the cluster from the analyzers dataset). There is a general  
304 agreement between the clusters from the analyzers and the ones from the sensors. Each cluster pair  
305 contains roughly the same number of points (Table 1 and Table 2). This 1-to-1 correspondence  
306 allows a direct comparison of the two sets of results.





307

308 **Fig. 6.** Graphical comparison of clustering results (K=7) between dataset 1 (analyzers) and dataset 2  
 309 (sensors)

310

311 For instance, cluster 1 (vent. OFF), cluster 4 (NO+NO<sub>2</sub>) and cluster 5 (NO<sub>2</sub>) match very well each  
 312 other, with only a few mismatched points. These clusters are associated to a well defined event,  
 313 respectively ventilation OFF, NO+NO<sub>2</sub> release, and NO<sub>2</sub> injection, that is perfectly singled out by  
 314 the K-means procedure, leading to an overlap ratio between dataset 2 and dataset 1 higher than 91  
 315 % for cluster 1, and of 98% for clusters 4 and 5. Only about 8% of the datapoints of sensors cluster  
 316 1 are associated to the reference cluster 2 (ventilation ON), though no explanation can be advanced.  
 317 The agreement between the two datasets is slightly poorer for cluster 2 and 3 (vent. ON). The data  
 318 are split between their respective reference clusters. This might be explained by the relatively low  
 319 NO<sub>2</sub> and O<sub>3</sub> concentration amplitudes and the cross sensitivity of the NO-B4, NO<sub>2</sub>-B4 and O<sub>3</sub>-B4  
 320 sensors [47]. 393 observations are mismatched and associated to the period without ventilation  
 321 (cluster 1). Cluster 6 (CO<sub>2</sub> vent. OFF) and cluster 7 (CO<sub>2</sub> vent. ON) from the sensors dataset are  
 322 also mainly divided through the two clusters of dataset 1 that describe the high CO<sub>2</sub> concentration  
 323 periods (analyzers clusters 6 and 7), leading to overlaps of 66% at most. We assigned this weaker

324 agreement to the low NO<sub>2</sub> and O<sub>3</sub> concentration, which do not allow for a good differentiation  
 325 between the ON and OFF ventilation conditions.

326

327 **Table 3** Overlap between the two sets of clusters

Reference Sensors	Cluster 1 (vent. OFF)	Cluster 2 (vent. ON)	Cluster 3 (vent. ON)	Cluster 4 (NO+NO <sub>2</sub> )	Cluster 5 (NO <sub>2</sub> )	Cluster 6 (CO <sub>2</sub> OFF)	Cluster 7 (CO <sub>2</sub> ON)
Cluster 1 (vent. OFF)	<b>91.1%</b>	<b>23.0%</b>	1.5%	0.0%	0.0%	0.4%	5.0%
Cluster 2 (vent. ON)	<b>7.9%</b>	<b>37.1%</b>	<b>30.4%</b>	2.2%	0.0%	0.0%	1.3%
Cluster 3 (vent. ON)	0.9%	<b>39.4%</b>	<b>66.1%</b>	0.0%	1.6%	0.0%	<b>9.3%</b>
Cluster 4 (NO+NO <sub>2</sub> )	0.0%	0.0%	0.0%	<b>97.8%</b>	0.0%	0.0%	0.0%
Cluster 5 (NO <sub>2</sub> )	0.0%	0.0%	0.1%	0.0%	<b>98.4%</b>	0.0%	0.0%
Cluster 6 (CO <sub>2</sub> OFF)	0.0%	0.1%	0.0%	0.0%	0.0%	<b>48.4%</b>	<b>18.3%</b>
Cluster 7 (CO <sub>2</sub> ON)	0.1%	0.4%	1.9%	0.0%	0.0%	<b>51.3%</b>	<b>66.3%</b>

328

329 Because of this similarities and links between clusters 2 and 3 and clusters 6 and 7 respectively, it is  
 330 natural to simplify the data distribution into 5 different classes by grouping some clusters together.

331 Thus, class 1 describes the indoor condition when the ventilation is off, with only the data from  
 332 cluster 1. Class 2 is composed of cluster 2 and cluster 3, corresponding to the ventilated periods.

333 Class 3 describes the combined increase of NO and NO<sub>2</sub> concentration of cluster 4. Class 4  
 334 describes the injection of NO<sub>2</sub> inside the room (cluster 5). Finally, class 5 (cluster 6 + cluster 7)

335 describes the period with high CO<sub>2</sub> concentration, either from controlled CO<sub>2</sub> injection or from the  
 336 presence of people in the room. Table 4 summarizes the overlap ratio calculated between the 5  
 337 classes defined by the clustering results on reference analyzers (dataset 1) and sensor measurements  
 338 (dataset 2). The overlap ratios are at least 87.6% for class 2, and up to 98.4% for class 4. Only class  
 339 1 and 2 still are slightly mingled, with up to 11% of mismatched data. Class 5 also presents about  
 340 6% of mismatched data, principally falling on class 2. This illustrates that the K-means procedure,  
 341 while allowing to identify the events, is not able to pick up correctly the transition between the two  
 342 baseline cases (ventilation ON and ventilation OFF), probably because this transition actually could  
 343 or should be represented by an additional cluster, as already discussed in the analysis of dataset 1,  
 344 nor the difference between the end of the CO<sub>2</sub> injection events, with only residual concentration that  
 345 are also not clearly distinguished from the baseline case.

346

347 **Table 4** Overlap ratio between 5 classes of dataset 2 and dataset 1

Reference Sensors	Class 1 (vent. OFF)	Class 2 (vent ON)	Class 3 (NO+NO <sub>2</sub> )	Class 4 (NO <sub>2</sub> )	Class 5 (CO <sub>2</sub> )
Class 1 (vent. OFF)	<b>91.1%</b>	<b>11.1%</b>	0.0%	0.0%	3.1%
Class 2 (vent ON)	<b>8.8%</b>	<b>87.6%</b>	2.2%	1.6%	<b>6.2%</b>
Class 3 (NO+NO <sub>2</sub> )	0.0%	0.0%	<b>97.8%</b>	0.0%	0.0%
Class 4 (NO <sub>2</sub> )	0.0%	0.0%	0.0%	<b>98.4%</b>	0.0%
Class 5 (CO <sub>2</sub> )	0.1%	1.3%	0.0%	0.0%	<b>90.7%</b>

348

349

#### 350 **4 Conclusions**

351 The present work demonstrates that low-cost sensors are able to detect specific air quality events  
352 occurring inside a room, and that these events can be classified without supervision using a K-  
353 means clustering procedure. The identification of these events requires some outside knowledge, as  
354 provided by the log of the experiments, or by the expertise of the user. When applying the K-means  
355 classification procedure to the data from the reference online gas analyzers, we were able to  
356 discriminate the normal ventilation pattern ON/OFF inside the room, and the artificial events such  
357 as CO<sub>2</sub> or NO<sub>2</sub> voluntary injections, as well as a NO and NO<sub>2</sub> unintentional spill. Applying the K-  
358 means procedure to the signals from the sensors as input leads to the same results, with a really  
359 good agreement with the analyzers, as shown by the overlap analysis. Based on the measured  
360 components (CO<sub>2</sub>, NO, NO<sub>2</sub> and O<sub>3</sub>), two sets of two clusters were not so well determined, possibly  
361 because of low NO<sub>2</sub> and O<sub>3</sub> concentration. Merging these two groups of clusters into two classes  
362 provides a much better agreement between the reference data (analyzers) and the sensors, with an  
363 overlap ratio higher than 88%.

364 The unsupervised classification does not require that the sensors be calibrated before the  
365 experiment, or that the chemical interferences be studied beforehand. This is a definite advantage  
366 towards a generalized deployment of sensors in buildings for the operative management of the  
367 ventilation and filtration systems, when quantitative measurements are not critical. Should absolute  
368 quantitative measurements be needed, the present methodology would still be applicable, but would  
369 require that the metrological performances of the sensors be established prior to the deployment.

370 The current efforts from manufacturers and research groups to improve the performances of the  
371 sensors, both on the short and on the long term, will be determinant to reach this objective.

372 The mathematical procedure we have developed could certainly be improved, in particular with  
373 respect to the automatic determination of the optimal number of classes, which so far needs to be  
374 defined beforehand or to be adjusted by the expert, using either criteria about the stability of the

375 clusters when their number is increased, or contextual information to supplement the signals from  
376 the sensors. In addition, using this unsupervised analysis of the signals from the sensors in different  
377 real or realistic conditions, it could be possible to construct a set of classes representative of various  
378 IAQ events. The resulting database would be used as a guide for the interpretation of the monitored  
379 events, and as input for a supervised classification model, which would render easy and efficient the  
380 management of IAQ with sensors installed in buildings. Measurements in real conditions in various  
381 buildings are currently underway, and will be used to further validate the classification methodology  
382 proposed here, and to establish such a database of “chemical signature” associated with specific  
383 IAQ events.

384

385

### 386 **Acknowledgments**

387 The authors would like to thank the French Environment and Energy Management Agency ADEME  
388 (Agence de l'Environnement et de la Maîtrise de l'Energie) for their financial support of the  
389 MERMAID project (PRIMEQUAL Program). This work is a contribution to the CaPPA project  
390 (Chemical and Physical Properties of the Atmosphere), funded by the French National Research  
391 Agency (ANR) through the PIA (Programme d'Investissement d'Avenir) under contract ANR-11-  
392 LABX-005-01, and a contribution to the CPER research project CLIMIBIO, with financial support  
393 from the French Ministère de l'Enseignement Supérieur et de la Recherche, the Hauts de France  
394 Region and the European Funds for Regional Economical Development.

395

396

397

398

### 399 **References**

- 400 [1] G.A. Ayoko, H. Wang, *Volatile Organic Compounds in Indoor Environments*, Indoor Air  
401 Pollution, Springer, Berlin, Heidelberg, 2014: pp. 69–107. doi:10.1007/698\_2014\_259.
- 402 [2] G. Buonanno, L. Morawska, L. Stabile, Particle emission factors during cooking activities,  
403 Atmospheric Environment 43 (2009) 3235–3242. doi:10.1016/j.atmosenv.2009.03.044.
- 404 [3] K.W. Tham, Indoor air quality and its effects on humans—A review of challenges and  
405 developments in the last 30 years, Energy and Buildings 130 (2016) 637–650.  
406 doi:10.1016/j.enbuild.2016.08.071.
- 407 [4] G. Buonanno, F.C. Fuoco, A. Russi, L. Stabile, Individual exposure of women to fine and  
408 coarse PM, Environmental Engineering and Management Journal 14 (2015) 827–836.  
409 doi:10.30638/eemj.2015.092.
- 410 [5] M. Verrielle, C. Schoemaeker, B. Hanoune, N. Leclerc, S. Germain, V. Gaudion, N. Locoge,  
411 The Mermaid Study: Indoor and Outdoor Average Pollutant Concentrations in 10 Low-Energy  
412 School Buildings in France, Indoor Air. 26 (2016) 702–713. doi:10.1111/ina.12258.
- 413 [6] N. Castell, F.R. Dauge, P. Schneider, M. Vogt, U. Lerner, B. Fishbain, D. Broday, A.  
414 Bartonova, Can commercial low-cost sensor platforms contribute to air quality monitoring and  
415 exposure estimates?, Environment International. 99 (2017) 293–302.  
416 doi:10.1016/j.envint.2016.12.007.
- 417 [7] A.C. Lewis, J.D. Lee, P.M. Edwards, M.D. Shaw, M.J. Evans, S.J. Moller, K.R. Smith, J.W.  
418 Buckley, M. Ellis, S.R. Gillot, A. White, Evaluating the performance of low cost chemical  
419 sensors for air pollution research, Faraday Discuss. 189 (2016) 85–103.  
420 doi:10.1039/C5FD00201J.
- 421 [8] P. Kumar, A.N. Skouloudis, M. Bell, M. Viana, M.C. Carotta, G. Biskos, L. Morawska, Real-  
422 time sensors for indoor air monitoring and challenges ahead in deploying them to urban  
423 buildings, Science of The Total Environment. 560–561 (2016) 150–159.  
424 doi:10.1016/j.scitotenv.2016.04.032.

- 425 [9] A. Caron, B. Hanoune, N. Redon, P. Coddeville, Gas sensor networks: relevant tools for real-  
426 time indoor air quality indicators in low energy buildings, in: Proceedings of the Healthy  
427 Buildings Europe 2015 Conference, 2015.
- 428 [10] F. Röck, N. Barsan, U. Weimar, Electronic nose: current status and future trends, *Chemical*  
429 *Reviews*. 108 (2008) 705–725.
- 430 [11] G. Neri, First Fifty Years of Chemosistive Gas Sensors, *Chemosensors*. 3 (2015) 1–20.  
431 doi:10.3390/chemosensors3010001.
- 432 [12] M. Aleixandre, M. Gerboles, Review of small commercial sensors for indicative monitoring of  
433 ambient gas, *Chemical Engineering Transactions*. 30 (2012) 169–174.
- 434 [13] B. Szulczyński, J. Gębicki, Currently Commercially Available Chemical Sensors Employed  
435 for Detection of Volatile Organic Compounds in Outdoor and Indoor Air, *Environments*. 4  
436 (2017) 21. doi:10.3390/environments4010021.
- 437 [14] A. Caron, N. Redon, F. Thevenet, B. Hanoune, P. Coddeville, Performances and limitations of  
438 electronic gas sensors to investigate an indoor air quality event, *Building and Environment*.  
439 107 (2016) 19–28. doi:10.1016/j.buildenv.2016.07.006.
- 440 [15] X. Pang, M.D. Shaw, A.C. Lewis, L.J. Carpenter, T. Batchellier, Electrochemical ozone  
441 sensors: A miniaturised alternative for ozone measurements in laboratory experiments and air-  
442 quality monitoring, *Sensors and Actuators B: Chemical*. 240 (2017) 829–837.  
443 doi:10.1016/j.snb.2016.09.020.
- 444 [16] L. Spinelle, M. Gerboles, M.G. Villani, M. Aleixandre, F. Bonavitacola, Field calibration of a  
445 cluster of low-cost commercially available sensors for air quality monitoring. Part B: NO, CO  
446 and CO<sub>2</sub>, *Sensors and Actuators B: Chemical*. 238 (2017) 706–715.  
447 doi:10.1016/j.snb.2016.07.036.
- 448 [17] W. Jiao, G. Hagler, R. Williams, R. Sharpe, R. Brown, D. Garver, R. Judge, M. Caudill, J.  
449 Rickard, M. Davis, L. Weinstock, S. Zimmer-Dauphinee, K. Buckley, Community Air Sensor

- 450 Network (CAIRSENSE) project: evaluation of low-cost sensor performance in a suburban  
451 environment in the southeastern United States, *Atmospheric Measurement Techniques*. 9  
452 (2016) 5281–5292. doi:10.5194/amt-9-5281-2016.
- 453 [18] L. Spinelle, M. Aleixandre, M. Gerboles, Protocol of Evaluation and Calibration of Low-Cos  
454 Gas Sensors for the Monitoring of Air Pollution, (2013).  
455 [http://publications.jrc.ec.europa.eu/repository/bitstream/JRC83791/eur%20report%20protocol](http://publications.jrc.ec.europa.eu/repository/bitstream/JRC83791/eur%20report%20protocol%20evaluation.pdf)  
456 [%20evaluation.pdf](http://publications.jrc.ec.europa.eu/repository/bitstream/JRC83791/eur%20report%20protocol%20evaluation.pdf).
- 457 [19] P. Van Geloven, M. Honore, J. Roggen, S. Leppavuori, T. Rantala, The influence of relative  
458 humidity on the response of tin oxide gas sensors to carbon monoxide, *Sensors and Actuators*  
459 *B: Chemical*. 4 (1991) 185–188. doi:10.1016/0925-4005(91)80196-Q.
- 460 [20] J.H. Sohn, M. Atzeni, L. Zeller, G. Pioggia, Characterisation of humidity dependence of a  
461 metal oxide semiconductor sensor array using partial least squares, *Sensors and Actuators B:*  
462 *Chemical*. 131 (2008) 230–235. doi:10.1016/j.snb.2007.11.009.
- 463 [21] J.-E. Haugen, O. Tomic, K. Kvaal, A calibration method for handling the temporal drift of  
464 solid state gas-sensors, *Analytica Chimica Acta*. 407 (2000) 23–39. doi:10.1016/S0003-  
465 2670(99)00784-9.
- 466 [22] M.J. Fernández, J.L. Fontecha, I. Sayago, M. Aleixandre, J. Lozano, J. Gutiérrez, I. Gràcia, C.  
467 Cané, M. del C. Horrillo, Discrimination of volatile compounds through an electronic nose  
468 based on ZnO SAW sensors, *Sensors and Actuators B: Chemical*. 127 (2007) 277–283.  
469 doi:10.1016/j.snb.2007.07.054.
- 470 [23] A. Szczurek, M. Maciejewska, Recognition of benzene, toluene and xylene using TGS array  
471 integrated with linear and non-linear classifier, *Talanta*. 64 (2004) 609–617.  
472 doi:10.1016/j.talanta.2004.03.036.
- 473 [24] C. Bur, M. Bastuck, A. Lloyd Spetz, M. Andersson, A. Schütze, Selectivity enhancement of  
474 SIC-FET gas sensors by combining temperature and gate bias cycled operation using



- 475 multivariate statistics, *Sensors and Actuators B:Chemical* 193 (2014) 931-940.  
476 doi:10.1016/j.snb.2013.12.030.
- 477 [25] Y. González Martín, M.C. Cerrato Oliveros, J.L. Pérez Pavón, C. García Pinto, B. Moreno  
478 Cordero, Electronic nose based on metal oxide semiconductor sensors and pattern recognition  
479 techniques: characterisation of vegetable oils, *Analytica Chimica Acta.* 449 (2001) 69–80.  
480 doi:10.1016/S0003-2670(01)01355-1.
- 481 [26] S. De Vito, E. Esposito, M. Salvato, O. Popoola, F. Formisano, R. Jones, G. Di Francia,  
482 Calibrating chemical mutlisensory devices for real world applications: An in-depth comparison  
483 of quantitative machine learning approaches, *Sensors and Actuators B: Chemical.* 255 (2018)  
484 1191–1210. doi:10.1016/j.snb.2017.07.155.
- 485 [27] H.-K. Hong, H.W. Shin, H.S. Park, D.H. Yun, C.H. Kwon, K. Lee, S.-T. Kim, T. Moriizumi,  
486 Gas identification using micro gas sensor array and neural-network pattern recognition,  
487 *Sensors and Actuators B: Chemical.* 33 (1996) 68–71. doi:10.1016/0925-4005(96)01892-8.
- 488 [28] S.B. Kotsiantis, I.D. Zaharakis, P.E. Pintelas, Machine learning: a review of classification and  
489 combining techniques, *Artif Intell Rev.* 26 (2006) 159–190. doi:10.1007/s10462-007-9052-3.
- 490 [29] A. Olaode, G. Naghdy, C. Todd, Unsupervised classification of images: A review, *International*  
491 *Journal of Image Processing (IJIP).* 8 (2014) 325–342.
- 492 [30] S. Marco, A. Gutierrez-Galvez, Signal and data processing for machine olfaction and chemical  
493 sensing:A review, *IEEE Sensors Journal* 12 (2012) 3189-3214 doi:10.1109/jsen.2012.2192920.
- 494 [31] A. Hierlemann, R. Gutierrez-Osuna, Higher-order chemical sensing, *Chemical Reviews* 108.  
495 (2008) 563–613. doi:10.1021.cr068116m.
- 496 [32] M. Bicego, G. Tessari, G. Tecchiolli, M. Bettinelli, A comparative analysis of basic pattern  
497 recognition techniques for the development of small size electronic nose, *Sensors and*  
498 *Actuators B: Chemical.* 85 (2002) 137–144. doi:10.1016/S0925-4005(02)00065-5.

- 499 [33] T. Alizadeh, Chemiresistor sensors array optimization by using the method of coupled  
500 statistical techniques and its application as an electronic nose for some organic vapors  
501 recognition, *Sensors and Actuators B: Chemical*. 143 (2010) 740–749.  
502 doi:10.1016/j.snb.2009.10.018.
- 503 [34] K. Yan, D. Zhang, Feature selection and analysis on correlated gas sensor data with recursive  
504 feature elimination, *Sensors and Actuators B: Chemical*. 212 (2015) 353–363.  
505 doi:10.1016/j.snb.2015.02.025.
- 506 [35] J. Lei, C. Hou, D. Huo, Y. Li, X. Luo, M. Yang, H. Fa, M. Bao, J. Li, B. Deng, Detection of  
507 ammonia based on a novel fluorescent artificial nose and pattern recognition, *Atmospheric  
508 Pollution Research*. 7 (2016) 431–437. doi:10.1016/j.apr.2015.10.019.
- 509 [36] Z. Haddi, S. Mabrouk, M. Bougrini, K. Tahri, K. Sghaier, H. Barhoumi, N. El Bari, A. Maaref,  
510 N. Jaffrezic-Renault, B. Bouchikhi, E-Nose and e-Tongue combination for improved  
511 recognition of fruit juice samples, *Food Chemistry*. 150 (2014) 246–253.  
512 doi:10.1016/j.foodchem.2013.10.105.
- 513 [37] C. Hou, J. Li, D. Huo, X. Luo, J. Dong, M. Yang, X. Shi, A portable embedded toxic gas  
514 detection device based on a cross-responsive sensor array, *Sensors and Actuators B: Chemical*.  
515 161 (2012) 244–250. doi:10.1016/j.snb.2011.10.026.
- 516 [38] A.K. Jain, Data Clustering: 50 Years Beyond K-Means, *Pattern Recognition Letters*. 31 (2010)  
517 651–666. doi:10.1016/j.patrec.2009.09.011.
- 518 [39] M. Falasconi, M. Pardo, M. Vezzoli, G. Sberveglieri, Cluster validation for electronic nose  
519 data, *Sensors and Actuators B: Chemical*. 125 (2007) 596–606. doi:10.1016/j.snb.2007.03.004.
- 520 [40] H. Wu, T. Yue, Z. Xu, C. Zhang, Sensor array optimization and discrimination of apple juices  
521 according to variety by an electronic nose, *Anal. Methods*. 9 (2017) 921–928.  
522 doi:10.1039/C6AY02610A.

- 523 [41] M. Verma, M. Srivastava, N. Chack, A.K. Diswar, N. Gupta, A comparative study of various  
524 clustering algorithms in data mining, *International Journal of Engineering Research and*  
525 *Applications (IJERA)*. 2 (2012) 1379–1384.
- 526 [42] M. Steinbach, G. Karypis, V. Kumar, others, A Comparison of Document Clustering  
527 Techniques, in: *KDD Workshop on Text Mining*, Boston, 2000: pp. 525–526.
- 528 [43] S. Marshall, M.E. Celebi, Comparison of Conventional and Bisecting K-Means Algorithms on  
529 Color Quantization, in: *14th IASTED International Conference on Signal and Image*  
530 *Processing*, 2012. doi:10.2316/P.2012.786-041.
- 531 [44] J. Shen, S.I. Chang, E.S. Lee, Y. Deng, S.J. Brown, Determination of cluster number in  
532 clustering microarray data, *Applied Mathematics and Computation*. 169 (2005) 1172–1185.  
533 doi:10.1016/j.amc.2004.10.076.
- 534 [45] H. Yu, Z. Liu, G. Wang, An automatic method to determine the number of clusters using  
535 decision-theoretic rough set, *International Journal of Approximate Reasoning*. 55 (2014) 101–  
536 115. doi:10.1016/j.ijar.2013.03.018.
- 537 [46] M.M.-T. Chiang, B. Mirkin, Intelligent Choice of the Number of Clusters in K-Means  
538 Clustering: An Experimental Study with Different Cluster Spreads, *J Classif*. 27 (2010) 3–40.  
539 doi:10.1007/s00357-010-9049-5.
- 540 [47] L. Spinelle, M. Gerboles, M.G. Villani, M. Aleixandre, F. Bonavitacola, Field calibration of a  
541 cluster of low-cost available sensors for air quality monitoring. Part A: Ozone and nitrogen  
542 dioxide, *Sensors and Actuators B: Chemical*. 215 (2015) 249–257.  
543 doi:10.1016/j.snb.2015.03.031.
- 544
- 545
- 546